JOC Article

An ab initio and Density Functional Theory Study of Radical-Clock Reactions

Christof M. Jäger, Matthias Hennemann, Andrzej Mieszała, and Timothy Clark*

Computer-Chemie-Centrum and Interdisciplinary Center for Molecular Materials, Friedrich-Alexander-Universität Erlangen-Nürnberg, Nägelsbachstrasse 25, 91052 Erlangen, Germany

clark@chemie.uni-erlangen.de

Received November 9, 2007

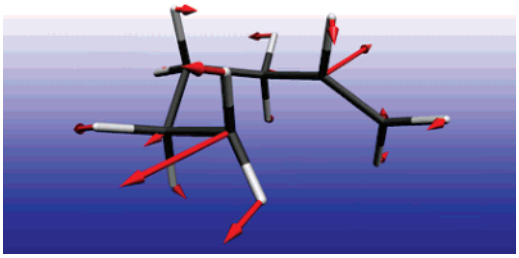

Density functional theory (DFT) and ab initio (CBS-RAD) calculations have been used to investigate a series of "radical clock" reactions. The calculated activation energies suggest that the barriers for these radical rearrangements are determined almost exclusively by the enthalpy effect with no evidence of significant polar effects. The ring-closure reactions to cyclopentylmethyl radical derivatives and the ring opening of cyclopropylmethyl radicals give different correlations between the calculated heat of reaction and barrier, but the two types of reaction are internally consistent.

Introduction

Radical clock reactions[1] have been a valuable tool in mechanistic research for more than 3 decades. Their use in classical physical organic mechanistic studies of radical reaction mechanisms was instrumental in attaining a consistent mechanistic picture of the factors governing radical reactivity.[2−9] As a consequence, radical clocks have also received some theoretical attention both with ab initio[10−13] and density functional theory (DFT)[12,14−18] methods. The central assumption of the radical-clock technique is that the rate of unimolecular radical rearrangement, either a ring closure or opening, is constant under all reaction conditions used. However, we[19] were recently able to show that the calculated activation energy for ring closing of the classical hex-1-en-6-yl radical[20] decreases very significantly when the double bond of the radical complexes a lithium cation. This effect found indirect experimental support from

(1) Griller, D.; Ingold, K. U. *Acc. Chem. Res.* **1980**, *13*, 317−323.
(2) Castellino, A. J.; Bruice, T. C. *J. Am. Chem. Soc.* **1988**, *110*, 7512−7519.
(3) Vanni, R.; Garden, S. J.; Banks, J. T.; Ingold, K. U. *Tetrahedron Lett.* **1995**, *36*, 7999−8002.
(4) Newcomb, M. *Tetrahedron* **1993**, *49*, 1151−1176.
(5) Ha, C.; Horner, J. H.; Newcomb, M.; Varick, T. R. *J. Org. Chem.* **1993**, *58*, 1194−1198.
(6) Newcomb, M.; Le Tadic-Biadatti, M-H.; Chestney, D. L.; Roberts, E. S.; Hollenberg, P. F. *J. Am. Chem. Soc.* **1995**, *117*, 12085−12091.
(7) Choi, S.-Y.; Eaton, P. E.; Hollenberg, P. F.; Liu, K. E.; Lippard, S. J.; Newcomb, M.; Putt, D. A.; Upadhyaya, S. P.; Xiong, Y. *J. Am. Chem. Soc.* **1996**, *118*, 6547−6555.
(8) Newcomb, M.; Choi, S.-Y.; Horner, J. H. *J. Org. Chem.* **1999**, *64*, 1225−1231.
(9) Valentine, A. M.; Le Tadic-Biadatti, M-H.; Toy, P. H.; Newcomb, M.; Lippard, S. J. *J. Biol. Chem.* **1999**, *274*, 10771−10776.
(10) Kemball, M. L.; Walton, J. C.; Ingold, K. U. *J. Chem. Soc., Perkin Trans.* **1982**, 2, *8*, 1017−1023.
(11) Hartung, J.; Stowasser, R.; Vitt, D.; Bringmann, G. *Angew. Chem., Int. Ed. Engl.* **1996**, *35*, 2820−2823.
(12) Maxwell, B. J.; Smith, B. J.; Tsanaktsidis, J. *J. Chem. Soc., Perkin Trans.* **2000**, *2*, 425−431.
(13) Chatagilialoglu, C.; Ferreri, C.; Lucarini, M.; Venturini, A.; Zavitsas, A. A. *Chem. Eur. J.* **1997**, *3*, 376−387.
(14) Wong, M. W.; Radom, L. *J. Phys. Chem.* **1995**, *99*, 8582−8588.
(15) Wong, M. W.; Radom, L. *J. Phys. Chem. A* **1998**, *102*, 2237−2245.
(16) Mayer, P. M.; Parkinson, C. J.; Smith, D. M.; Radom, L. *J. Chem. Phys.* **1998**, *108*, 604−615.
(17) Henry, D. J.; Parkinson, C. J.; Radom, L. *J. Phys. Chem. A* **2002**, *106*, 7927−7936.
(18) Smith, D. M.; Nicolaides, A.; Golding, B. T.; Radom, L. *J. Am. Chem. Soc.* **1998**, *120*, 10223−10233.
(19) Horn, A. H. C.; Clark, T. *J. Am. Chem. Soc.* **2003**, *125*, 2809−2816.
(20) (a) Brace, N. O. *J. Org. Chem.* **1967**, *32*, 2711. (b) Lal, D.; Griller, D.; Husband, S.; Ingold, K. U. *J. Am. Chem. Soc.* **1974**, *96*, 6355. (c) Schmid, P.; Griller, D.; Ingold, K. U. *Int. J. Chem. Kinet.* **1979**, *11*, 333. (d) Beckwith, A. L. J.; Easton, C. J.; Serelis, A. K. *J. Chem. Soc., Chem. Commun.* **1980**, 482.

10.1021/jo702421m CCC: $40.75
Published on Web 01/23/2008

TABLE 1. Radical Rearrangements Investigated with Available Experimental Reaction Rate Constants *k* and Activation Energies *E*

reaction		*k* [s^{-1}]	*E* [kcal mol^{-1}]	*ref.*
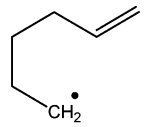 1	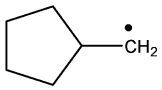 1P5	1.0×10^5 2.3×10^5	6.1	1, 4
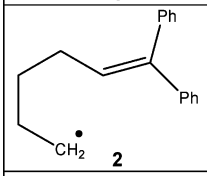 2	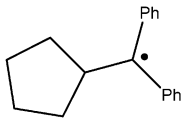 2P5	5.0×10^7	3.5	4, 5, 8
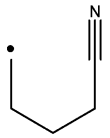 3	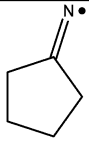 3P5	3.9×10^3	8.6	1
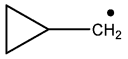 4	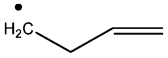 4P	1.3×10^8 9.4×10^7	5.9	1, 4
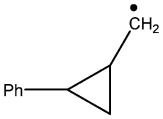 5	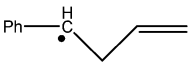 5P	3.0×10^{11} 4.0×10^{11} 1.8×10^{11}	3.5	4, 8, 9
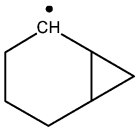 6	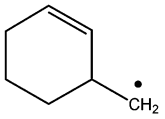 6P6	2.0×10^8		30, 31, 33
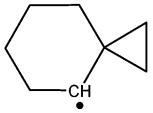 7	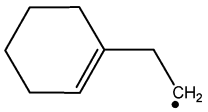 7P6	5.0×10^7		33

Michl's recent work[21,22] in which "naked" Li^+ was shown to catalyze the radical polymerization of terminal olefins, in accord with proposal made 20 years ago on the basis of ab initio calculations[23] and a recent more detailed study at higher theoretical levels.[24]

We now report a survey of radical clock reactions at the DFT and ab initio levels of theory. The purpose of this work is two-fold: we wish to evaluate the existing theoretical understanding of the factors affecting radical clock rearrangement rates and to report calculated data on the unperturbed reactions with which we can later compare those for the same reactions coordinated to metal or halide ions or confined in model enzyme active sites. The systems investigated and a summary of their most important experimental data are shown in Table 1.

Methods

All calculations used the Gaussian03 suite of programs.[25] Initial geometry optimizations were performed using the B3LYP[26] hybrid density functional and the 6-31G(d) basis set.[27] Minima and transition states were confirmed as such by calculating their normal vibrations at this level of theory. The zero-point energies derived from these calculations were used for the CBS-RAD-(QCISD, B3LYP) calculations.[14,15] For all but the largest systems, further optimizations at the QCISD/6-31G(d)[28] level were also performed. To obtain the CBS-RAD energies, further

(21) Vyakaranam, K.; Barbour, J. B.; Michl, J. *J. Am. Chem. Soc.* **2006**, *128*, 5610−5611.
(22) Vyakaranam, K.; Körbe, S.; Michl, J. *J. Am. Chem. Soc.* **2006**, *128*, 5680−5686.
(23) Clark, T. *J. Chem. Soc., Chem. Commun.* **1986**, 1774−1775.
(24) Clark, T. *J. Am. Chem. Soc.* **2006**, *128*, 11278−11285.
(25) Frisch, M. J. et al. *Gaussian 03*; Gaussian, Inc.: Pittsburgh PA, 2003.
(26) Becke, A. D. *J. Chem. Phys.* **1993**, *98*, 1372. Becke, A. D. *J. Chem. Phys.* **1993**, *98*, 5648. Stephens, P. J.; Devlin, F. J.; Chabalowski, C. F.; Frisch, M. J. *J. Phys. Chem.* **1994**, *98*, 11623. Becke, A. D. *J. Chem. Phys.* **1993**, *98*, 5648. Becke, A. D. In *The Challenge of d- and f-Electrons: Theory and Computation*; Salahub, D. R., Zerner, M. C., Eds.; American Chemical Society: Washington, DC, 1989; Chapter 12, pp 165−179. Vosko, S. H.; Wilk, L.; Nusait, M. *Can. J. Phys.* **1980**, *58*, 1200. Lee, C.; Yang, W.; Parr, R. G. *Phys. Rev. B* **1988**, *37*, 785.

CHART 1. Overview of the Structures Investigated for 1

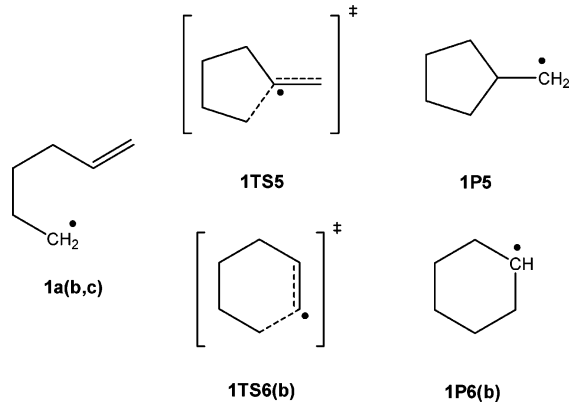

TABLE 2. Calculated Relative Energies for the Radical Rearrangement of 1[a]

	B3LYP/6-31G(d)	QCISD/6-31G(d)	CBS-RAD (QCISD,B3LYP)
1	0.0	0.0	0.0
1a	1.7	1.6	2.1
1b	1.4	1.5	1.4
1c	3.9	3.7	4.1
1P5	−13.3	−15.4	−14.5
1TS5	9.4	11.8	8.3
1TS5b	7.7	10.3	6.9
1P6	−20.4	−21.7	−19.7
1P6b	−16.4	−17.5	−15.5
1TS6	10.2	12.5	9.4
1TS6b	12.6	14.9	12.1

[a] All relative energies are given in kcal mol^{-1}. Absolute energies and S^2 values are given in Supporting Information. B3LYP/6-31G(d) and QCISD/6-31G(d) energy values are corrected with unscaled B3LYP/6-31-G(d) zero point energies.

single point energy calculations were performed, and the energies were calculated according to the procedure outlined by Radom and co-workers.[16]

Results

Ring Closures to Cyclopentylmethyl Radicals. Hex-1-en-6-yl Radical. We[19] and others[12] have reported CBS-RAD results for the parent hex-1-en-6-yl system. The extended conformation of radical **1**, which is calculated to be the most stable noncyclized conformation in the gas phase, forms different folded precursor conformations that can cyclize either to the observed cyclopentylmethyl radical product **1P5** or to the thermodynamically more stable cyclohexyl radical **1P6** (Chart 1).

In our previous work, we[19] described a reaction pathway for the 5-*exo*-cyclization to **1P5** via the precursor conformation **1a** and the transition state **1TS5**. However, detailed calculations revealed a different possible reaction pathway via the precursor conformation **1b** and the transition state **1TS5b**. Table 2 shows the calculated energies for this system. On the basis of these results, our best assessment for the activation energy of the

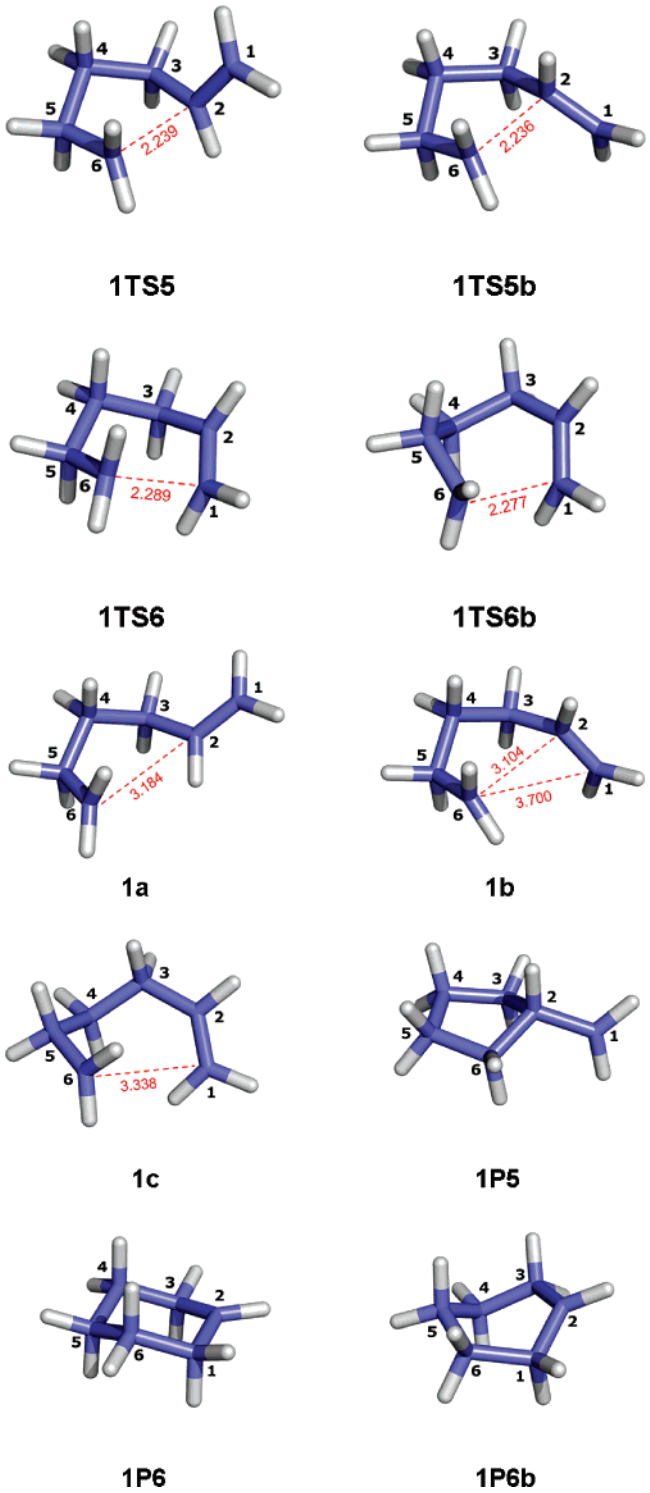

FIGURE 1. QCISD/6-31G(d)-optimized structures of **1** with bond-closing distances for the transition states.

cyclization to product **1P5** is 6.9 kcal mol^{-1} relative to the most stable conformation **1** or 5.5 kcal mol^{-1} relative to the precursor conformation **1b**. The geometries of the transition structures **1TS5** and **1TS5b** are very similar except for the orientation of the double bond (Figure 1). The QCISD/631G(d)-optimized ring-closure carbon−carbon distances in the transition state are 2.239 Å for **1TS5** and 2.236 Å for **1TS5b**.

Conformation **1b** also proved to be the precursor for the 6-*endo*-cyclization to the cyclohexyl radical **1P6** via the

(27) Ditchfield, R.; Hehre, W. J.; Pople, J. A. *J. Chem. Phys.* **1971**, *54*, 724. Hehre, W. J.; Ditchfield, R.; Pople, J. A. *J. Chem. Phys.* **1972**, *56*, 2257. Hariharan, P. C.; Pople, J. A. *Mol. Phys.* **1974**, *27*, 209. Gordon, M. S. *Chem. Phys. Lett.* **1980**, *76*, 163. Hariharan, P. C.; Pople, J. A. *Theor. Chim. Acta* **1973**, *28*, 213.
(28) Pople, J. A.; Head-Gordon, M.; Raghavachari, K. *J. Chem. Phys.* **1987**, *87*, 5968.

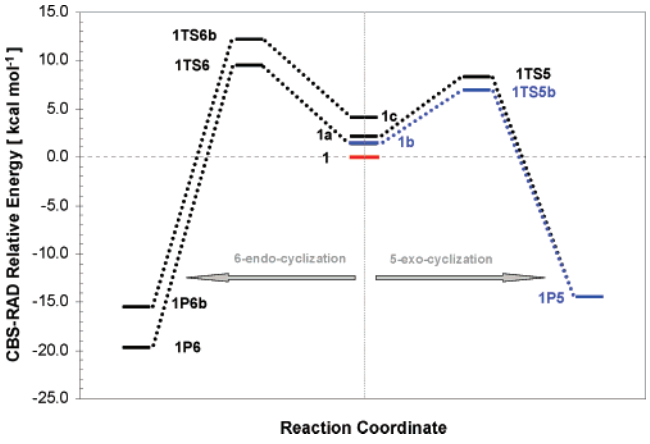

FIGURE 2. Schematic energy diagram of the radical rearrangement of **1**.

CHART 2. Overview of the Structures Investigated for 2

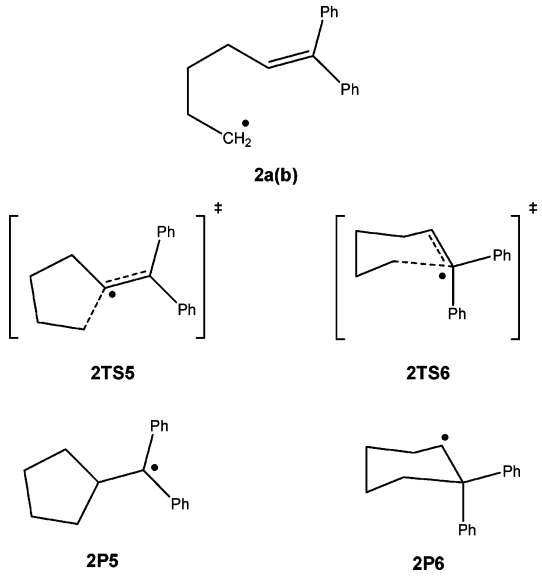

transition state **1TS6**. The activation energy for this radical rearrangement is 9.4 kcal mol^{-1} relative to **1** and 8.0 kcal mol^{-1} relative to **1b**. We also found another, less stable conformation, **1c**, that is the precursor for product **1P6b** and that has a more boat-like conformation of the cyclohexane ring, rather than the chair-like conformation of **1P6**. The energy of transition state **1TS6b** is 12.1 kcal mol^{-1} relative to **1** (Figure 2).

We have investigated two structural modifications of the hex-1-en-6-yl system for which experimental results are available. The 6,6-diphenyl derivative **2** and the 4-cyano-but-1-yl system **3**.

1,1,-Diphenyl-hex-1-en-6-yl Radical. The 1,1-diphenyl-hex-1-en-6-yl radical **2** is the largest system that we have investigated using DFT calculations. We were not able to perform geometry optimizations at the QCISD/631G(d) level. Therefore, we discuss the results of the B3LYP calculations. The resulting energy values have been corrected with unscaled B3LYP/6-31G(d) zero point energies.

Similar to the rearrangement of the hex-1-en-6-yl radical **1**, the extended conformation **2** is the most stable non-cyclized conformation in the gas phase and forms different precursor

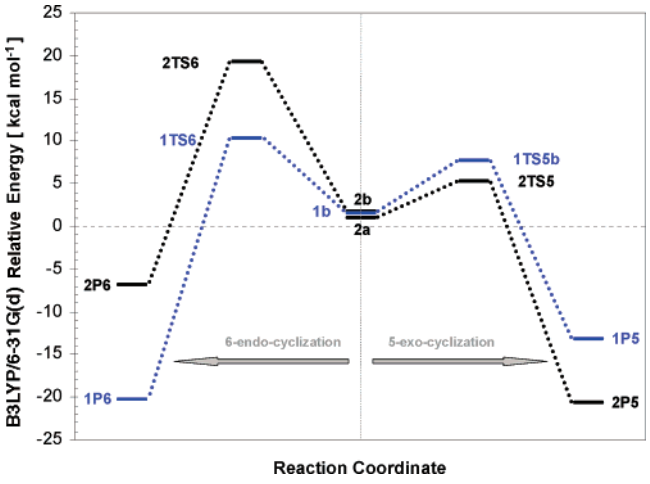

FIGURE 3. Schematic energy diagram of the radical rearrangement of **2** in comparison with that of **1**, both at the B3LYP/6-31G(d) level of theory. The energy values are corrected with unscaled B3LYP/6-31G(d) zero point energies.

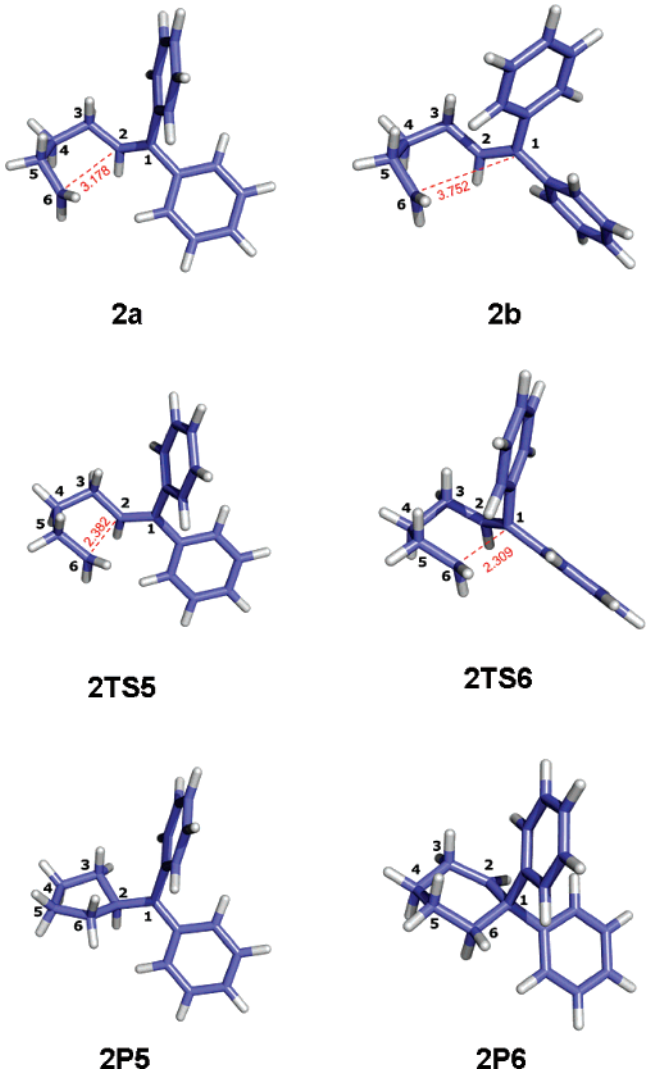

FIGURE 4. B3LYP/6-31G(d)-optimized structures of **2** with bond-closing distances for the transition states.

conformations for the ring-closure rearrangements (Chart 2). Figure 4 shows the optimized structures obtained for the

TABLE 3. Calculated Relative Energies for the Radical Rearrangements of 2 and 3[a]

	B3LYP/6-31G(d)	QCISD/6-31G(d)	CBS-RAD (QCISD,B3LYP)
2	0.0		
2a	1.0		
2b	1.6		
2P5	−20.7		
2TS5	5.3		
2P6	−6.9		
2TS6	19.2		
3	0.0	0.0	0.0
3a	1.0	0.8	2.2
3P5	−10.3	−8.9	−7.4
3TS5	9.0	12.0	10.5
3P6	4.8	9.2	8.0
3TS6	19.0	23.2	21.4

[a] All relative energies are given in kcal mol^{-1}. Absolute energies and S^2 values are given in Supporting Information. B3LYP/6-31G(d) and QCISD/6-31G(d) energy values are corrected with unscaled B3LYP/6-31-G(d) zero point energies.

CHART 3. Overview of the Structures Investigated for 3

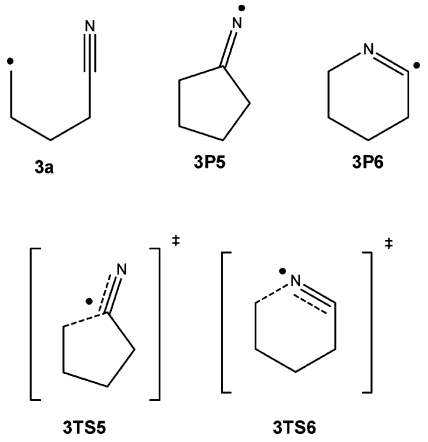

rearrangement of **2**. The most stable precursor conformation **2a** is part of the ring-closure reaction pathway to the cyclopentyl product **2P5** via the transition state **2TS5**, whereas the precursor **2b** forms the cyclohexyl product **2P6** via transition state **2TS6**. The two precursors are only 0.6 kcal mol^{-1} apart in energy and have similar structures. The important C−C distances for the ring-closing rearrangements are almost identical. The distances between C6 and C2 are 3.178 Å for **2a** and 3.110 Å for **2b**, and the C6−C1 distances are 3.753 and 3.752 Å. The only differences in the two structures are the dihedral angles governing the orientation of the planar phenyl rings toward the double bond (C1−C2). Steric hindrance means that the phenyl rings cannot rotate freely, and it is therefore possible to discriminate between the two precursors. The dihedral angles differ by 116.8° for the phenyl rings in *cis*-position to C3 and 73.7° for the *trans* phenyl rings. This difference influences the ability for the precursor **2b** to rearrange to the 6-*endo* product **2P6**. The C−C ring-closure distances are 2.382 Å in transition state **2TS5** and 2.309 Å in **2TS6**.

The calculated activation energies at the B3LYP level are 5.3 kcal mol^{-1} for the cyclization to **2P5** and 19.2 kcal mol^{-1} for that to **2P6**. The ring closure to the substituted cyclohexyl radical **2P6** is thus even more unlikely than in the parent system (to give **1P6**), whereas the ring closure to the cyclopentyl radical **2P5** shows an activation barrier lower than that of the parent

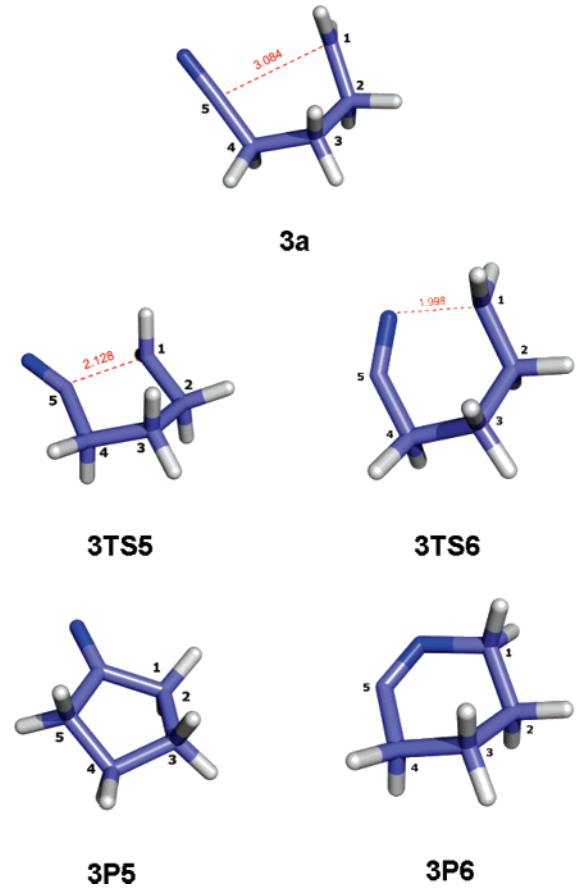

FIGURE 5. QCISD/6-31G(d)-optimized structures of **3** with bond-closing distances for the transition states.

CHART 4. Overview of the Structures Investigated for 4 and 5

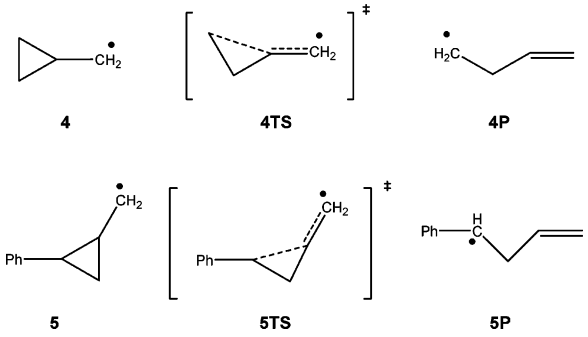

reaction. This result agrees well with experimental results, which suggest activation energies of 6.1 kcal mol^{-1} for the rearrangement of **1** and 3.5 kcal mol^{-1} for that of **2**.[1,8] A schematic comparison of the results of system **2** with those of system **1** are shown in Figure 3. The relative energies are listed together with the results of system **3** in Table 3.

4-Cyano-but-1-yl Radical, 3. The second structural modification of the hex-1-en-6-yl system investigated is the 4-cyano-but-1-yl system **3**.

We analyzed the two possible ring-closure rearrangements to the products **3P5** and **3P6** (Chart 3). Again, the extended conformation **3** is the most stable acyclic conformation. Further, we found the one precursor conformation **3a** for both rear-

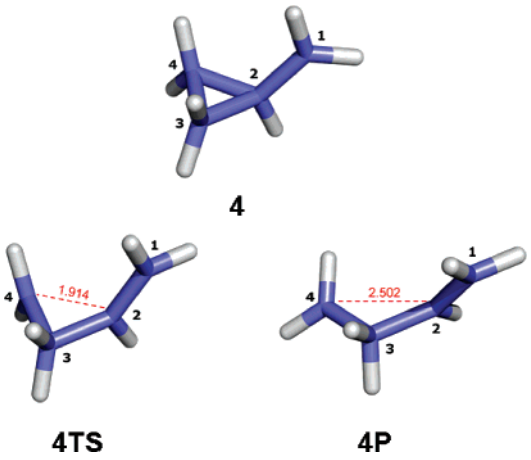

FIGURE 6. QCISD/6-31G(d)-optimized structures of **4** with bond closing distances for the transition states.

rangements. The two ring-closure transition states **3TS5** and **3TS6** are shown in Figure 5.

We analyzed the two possible ring-closure rearrangements to the products **3P5** and **3P6**. Again, the extended conformation **3** is the most stable acyclic conformation. Further, we found one precursor conformation **3a** for both rearrangements. The two ring-closure transition states **3TS5** and **3TS6** are shown in Figure 5.

The CBS-RAD activation energies are 10.5 kcal mol^{-1} for the ring closure to give the five-membered ring product **3P5** and 21.4 kcal mol^{-1} to form the 6-*endo* alternative **3P6**.

The geometries of the two ring-closure paths are very similar. The transition state distances from the QCISD/6-31G(d) geometry optimizations are 2.128 Å for the C−C bond formation of **3TS5** and 1.998 Å for the C−N bond formation of **3TS6**.

In agreement with experimental results[1] the calculated activation barrier for ring closure of the 4-cyano-but-1-yl radical is higher than those for the other radical clock systems **1** and **2**.

Ring Opening of Cyclopropylcarbinyl Radicals. Cyclopropylcarbinyl. Faster radical clocks than the cyclopentylcarbinyl systems discussed above use the ring opening of cyclopropylcarbinyl radicals as the characteristic rearrangement.[4] We have considered four different radical clocks of this type (**4**−**7**) and their possible ring-opening reactions.

The radicals **4** and **5** (Chart 4) represent two different substituted cyclopropane probes for which experimental results of the radical clock behavior are available.[9,29]

Radical **4** rearranges to product **4P** via the transition state **4TS** (Figure 6). The CBS-RAD-calculated activation energy is 7.2 kcal mol^{-1}. Two different low energy conformations were found for radical **5**. Structures **5a** and **5b** differ in the configuration of C2, which leads to different orientations of the methyl radical group toward the phenyl ring, as shown in Figure 7. The two diastereomers differ slightly in energy. The (*R*,*R*)-conformer **5a** is approximately 1.4 kcal mol^{-1} more stable than the (*S*,*R*)-diastereomer **5b** at the CBS-RAD level. Conformer **5a** rearranges to product **5P** via transition state **5TS.** The CBS-RAD-calculated activation energy is 4.4 kcal mol^{-1}. For the (*S*,*R*)-diastereomer **5b** the rearrangement (via **5TSb** to give **5Pb**) has a barrier of 4.6 kcal mol^{-1} relative to **5a** and 3.0 kcal mol^{-1} relative to **5b**. The QCISD/6-31G(d)- calculated interatomic

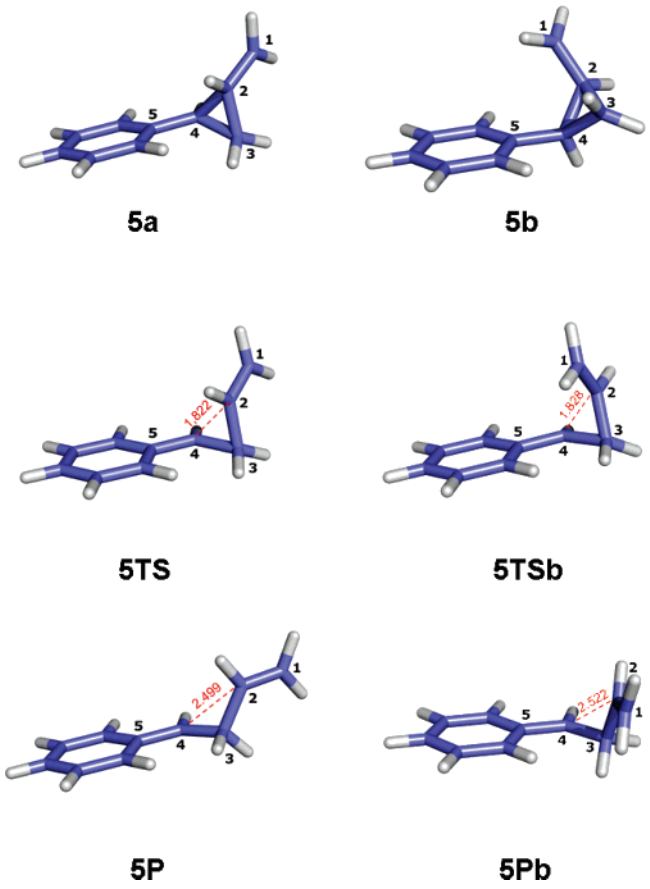

FIGURE 7. QCISD/6-31G(d)-optimized structures of **5** with bond closing distances for the transition states.

TABLE 4. Calculated Relative Energies for the Radical Rearrangements of 4 and 5[a]

	B3LYP/6-31G(d)	QCISD/6-31G(d)	CBS-RAD (QCISD,B3LYP)
4	0.0	0.0	0.0
4P	−3.1	−3.4	−3.0
4TS	7.6	10.6	7.2
5a	0	0.0	0.0
5P	−14.3	−11.6	−12.8
5TS	1.5	7.8	4.4
5b	1.9	0.4	1.6
5Pb	−13.7	−11.5	−11.5
5TSb	3.4	9.6	4.6

[a] All relative energies are given in kcal mol^{-1}. Absolute energies and S^2 values are given in Supporting Information. B3LYP/6-31G(d) and QCISD/6-31G(d) energy values are corrected with unscaled B3LYP/6-31-G(d) zero point energies.

distances for the cyclopropane ring opening are 1.914 Å in **4TS**, 1.822 in **5TS**, and 1.828 Å in **5TSb**.

Norcarane. Newcomb et. al,[30,31] Groves and co-workers,[32,33] and others have investigated the behavior of the radical clocks norcarane **6** and spirooctane **7** experimentally. They pointed out

(29) Martin-Esker, A. A.; Johnson, C. C.; Horner, J. H.; Newcomb, M. *J. Am. Chem. Soc.* **1994**, *116*, 9174−9181.

(30) Newcomb, M.; Shen, R.; Lu, Y.; Coon, M. J.; Hollenberg, P. F.; Kopp, D. A.; Lippard, S. J. *J. Am. Chem. Soc.* **2002**, *124*, 6879−6886.

(31) Chatgilialoglu, C.; Newcomb, M. *Adv. Organomet. Chem.* **1999**, *44*, 67−112.

(32) Brazeau, B. J.; Austin, R. N.; Tarr, C.; Groves, J. T. *J. Am. Chem. Soc.* **2001**, *123*, 11831−11837.

(33) Auclair, K.; Hu, Z.; Little, D. M.; Ortiz de Montellane, P. R.; Grooves, J. T. *J. Am. Chem. Soc.* **2002**, *124*, 6020−6027.

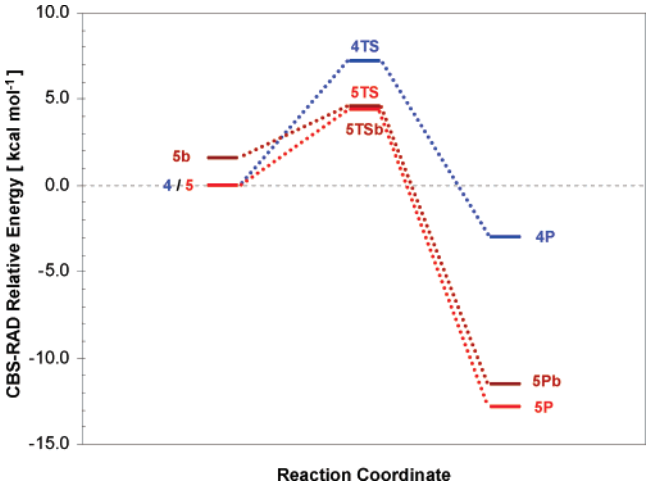

FIGURE 8. Schematic energy diagram of the radical rearrangements of **4** and **5**.

the ability of these probes to discriminate between radical and cationic intermediates, which give different rearrangement products. Chart 5 shows the different rearrangement paths for **6** and **7**. The radical rearrangements lead to the products **6P6** and **7P6** via the transition states **6TS6** and **7TS6**, whereas the alternative rearrangement leads to products **6P7** and **7P4** via transition states **6TS7** and **7TS4**. These alternative rearrangements are believed to proceed via cationic intermediates.[32] However, we have calculated them as radical rearrangements in order to be able to compare them with the competing rearrangement in the radical case.

We found two low energy conformations, **6a** and **6b**, for the norcarane radical **6**. The CBS-RAD-calculated energy difference between these two conformers is 1.4 kcal mol^{-1}. The conformations differ in the orientation of the ring position C4 (see Figure 9).

We found the most facile radical rearrangement of norcarane **6** to be the pathway starting from conformer **6a** via the transition state **6TS6a** to the product **6P6a**, which has a calculated (CBS-RAD) activation energy of 5.9 kcal mol^{-1}. The equivalent radical rearrangement pathway for the other conformer **6b** (via transition state **6TS6b** to give product **6P6b**) shows the same activation energy relative to conformer **6b** and 7.4 kcal mol^{-1} relative to **6a**. The geometries of the two transition states are very similar except for the ring position C4. The QCISD/6-31G(d) C−C interatomic distances for the ring opening are 1.915 Å for **6TS6a** and 1.918 Å for **6TS6b**.

The radical rearrangement of norcarane **6** to product **6P7** is less favorable. The activation barriers (CBS-RAD) are 10.7 kcal mol^{-1} for conformer **6a** and 9.3 kcal mol^{-1} for **6b** relative to **6a**. For this rearrangement, the transition state **6TS7b** is energetically more favorable than **6TS7a**. However, neither belongs to a low-energy pathway and they therefore do not represent possible radical rearrangements. The geometries of the transition state structures (Figure 9) indicate why **6TS7b** is lower in energy than **6TS7a**. The orientation of C4 in the more stable initial radical **6a** and the associated ring conformation affect the formation of the planar double bond in the ring system adversely.

Spirooctane. We found one low energy conformer for spirooctane **7** (Figure 11). The radical rearrangement follows the path via the transition state **7TS6** to the product **7P6**. The CBS-RAD activation energy is 6.9 kcal mol^{-1}, and the C−C

CHART 5. Overview of the Structures Investigated for 6 and 7

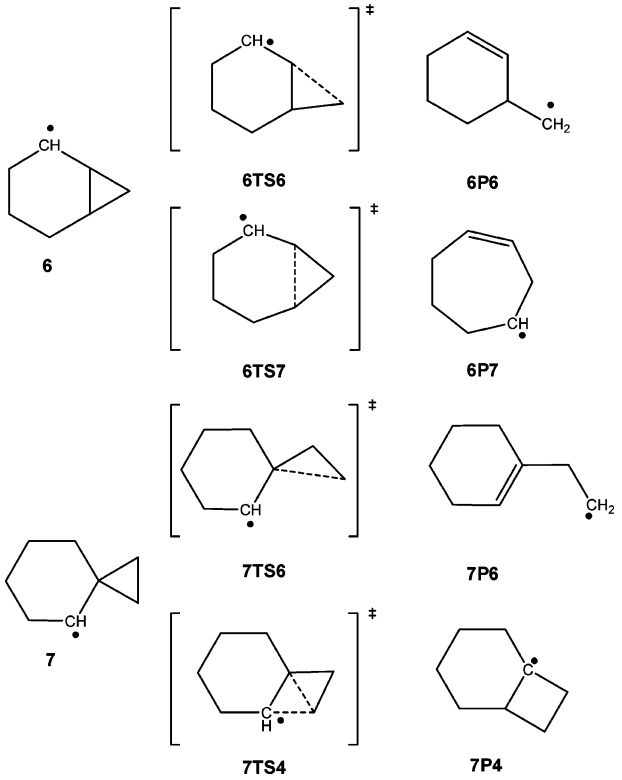

distance for the ring opening is 1.922 Å. The radical rearrangement to product **7P4**, which is suggested to arise via a cationic intermediate, has a very high activation barrier as it involves concerted bond formation and cleavage. The activation barrier at the CBS-RAD level is 46.5 kcal mol^{-1}, and the rearrangement is calculated to be endothermic by 1.6 kcal mol^{-1}. The C−C distances in the transition state **7TS4** are 1.778 Å for the cyclopropyl ring opening and 1.968 Å for the cyclobutane ring closure.

Discussion

Our first conclusion is the purely technical one that B3LYP/6-31G(d) results for these radical ring-opening and -closing reactions agree well with CBS-RAD, so that purely pragmatically B3LYP/6-31G(d) can be used as a fast and economical technique for investigating radical-clock reactions. This conclusion was suggested by our earlier work[19] but is confirmed here for a larger collection of radical clocks.

We can also assess the performance of the calculations by comparison with experiment. As rate constants are available for all of the reactions shown in Table 1 and also because these are the primary measured data rather than the experimental activation energies, which are derived from the temperature dependence of the measured rates, we have used the logarithms of the rate constants to compare with the calculated activation energies. Figure 13 shows the available data.

There is a good correlation ($R^2 = 0.932$) between log(k) and the CBS-RAD-calculated activation energies, as should be the case if the pre-exponential factor in the Arrhenius equation governing these reactions is constant. Neither the B3LYP/6-31G(d) nor the experimentally derived activation energies

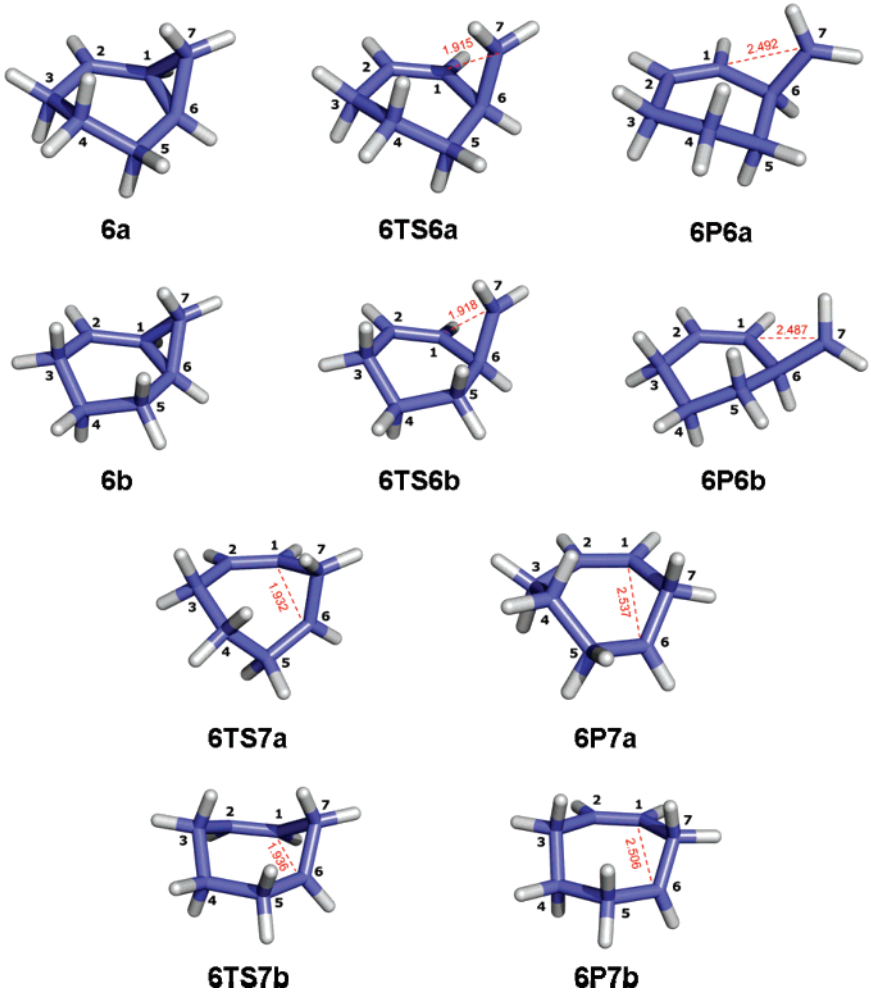

FIGURE 9. QCISD/6-31G(d)-optimized structures of **6** with bond-closing distances for the transition states.

TABLE 5. Calculated Relative Energies for the Radical Rearrangements of 6[a]

	B3LYP/6-31G(d)	QCISD/6-31G(d)	CBS-RAD (QCISD,B3LYP)
6a	0.0	0.0	0.0
6b	1.1	1.0	1.4
6P6a	−2.4	−3.2	−2.9
6TS6a	7.4	10.0	5.9
6P6b	−2.8	−3.5	−3.8
6TS6b	8.8	11.6	7.3
6P7a	−1.9	−1.4	−0.7
6TS7a	11.3	14.5	10.7
6P7b	−1.4	−1.5	−1.0
6TS7b	10.4	13.3	9.3

[a] All relative energies are given in kcal mol^{-1}. Absolute energies and S^2 values are given in Supporting Information. B3LYP/6-31G(d) and QCISD/6-31G(d) energy values are corrected with unscaled B3LYP/6-31-G(d) zero point energies.

TABLE 6. Calculated Relative Energies for the Radical Rearrangements of 7[a]

	B3LYP/6-31G(d)	QCISD/6-31G(d)	CBS-RAD (QCISD,B3LYP)
7	0	0	0
7P6	−5.2	−4.7	−5.4
7TS6	7.6	10.8	6.9
7P4	0.0	0.5	1.6
7TS4	47.5	52.5	46.5

[a] All relative energies are given in kcal mol^{-1}. Absolute energies and S^2 values are given in Supporting Information. B3LYP/6-31G(d) and QCISD/6-31G(d) energy values are corrected with unscaled B3LYP/6-31-G(d) zero point energies.

correlate as well with log(k). This suggests that the CBS-RAD-calculated activation energies are reliable, although there may be a systematic error. Radom et al.[34] have suggested that CBS-RAD consistently overestimates activation energies by 0.5−1 kcal mol^{-1}.

(34) Gomez-Balderas, R.; Coote, M. L.; Henry, D. J.; Radom, L. *J. Phys. Chem. A* **2004**, *108*, 2874−2883.

Linear regression of the experimental rate constants with the experimental and calculated activation energies gives eqs 1−3:

$$\log(k) = -30(7) + 2.7(1.2)\Delta E^*_{\text{experimental}}; \quad R^2 = 0.637,\ p = 0.11 \quad (1)$$

$$\log(k) = -27(4) + 1.8(0.6)\Delta E^*_{\text{B3LYP}}; \quad R^2 = 0.640,\ p = 0.030 \quad (2)$$

$$\log(k) = -37(3) + 3.0(0.4)\Delta E^*_{\text{CBS-RAD}}; \quad R^2 = 0.932,\ p = 0.002 \quad (3)$$

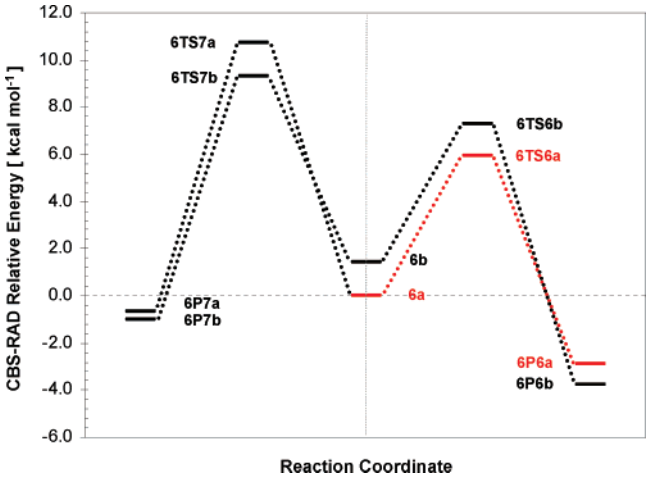

FIGURE 10. Schematic energy diagram of the radical rearrangement of **6**.

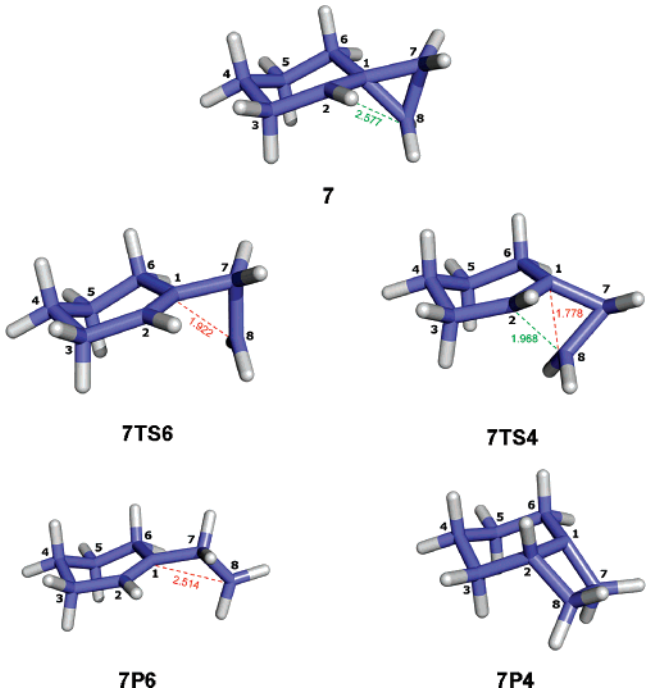

FIGURE 11. QCISD/6-31G(d)-optimized structures of **7** with bond-closing distances for the transition states.

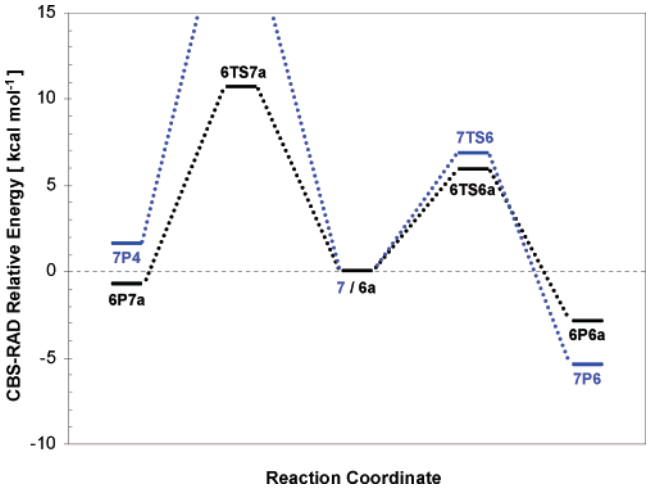

FIGURE 12. Schematic energy diagram of the radical rearrangement of **7** compared to the rearrangement of **6a**.

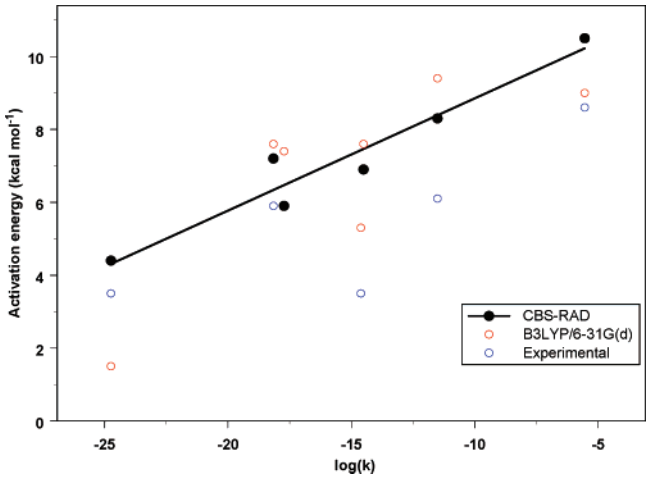

FIGURE 13. Plot of the calculated activation energies against the logarithm of the experimental rate constants. The experimental data are those given in Table 1. The line is the least-squares fit for the CBS-RAD calculations.

where ΔE^* represents the activation energy obtained by the method indicated in the subscript. As the standard deviation between predicted and observed log(k) values given by eq 3, which is by far the best of the correlations, is still 1.9 log units, we did not calculate absolute rate constants from the CBS-RAD data.

The final conclusion represents something of an anticlimax but also gives insight into the nature of these radical-clock reactions. Radical additions to multiple bonds are traditionally[35] believed to be influenced by polar effects that could conceivably affect the rates of radical-clock reactions. However, apart from the cyano system, the addition reactions involved in the radical clocks investigated here are all very similar in their electronic character, so that we might expect them not to vary widely in this respect. This has been assumed implicitly in the design of faster radical clocks, where more exothermic reactions were chosen as candidates for faster clocks. Our results allow us to test the relationship between heat of reaction and activation energy. Figure 14 shows the results for the ring-closing clocks, and Figure 15 shows the corresponding data for the ring-opening clocks.

Figure 14 shows that the QCISD/6-31G(d) results differ significantly from their B3LYP/6-31G(d) and CBS-RAD equivalents. This is probably a consequence of using the relatively small 6-31G(d) basis set with QCISD but may indicate that the correction for triple excitations plays a significant role in determining the calculated activation energies.

Otherwise, both figures show clearly that the calculated activation energies depend approximately linearly on the calculated heats of reaction. Using both the CBS-RAD and the

(35) Tedder, J. M. *Angew. Chem., Int. Ed. Engl.* **1982**, *21*, 401. Fischer, H.; Radom, L. *Angew. Chem., Int. Ed. Engl.* **2001**, *40*, 1340−1371.

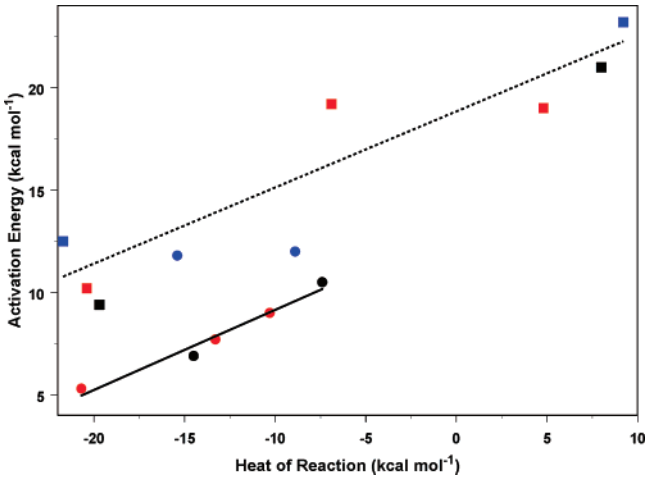

FIGURE 14. Plot of the calculated heats of reaction against the corresponding activation energies. Circles represent 5-*exo* cyclizations, and squares represent 6-*endo*. Black symbols give the CBS-RAD data, blue symbols give the QCISD data, and red symbols give the B3LYP data. The solid line is the least-squares fit for the 5-*exo* cyclizations excluding the QCISD results, the dashed line for all 6-*endo* cyclizations, including QCISD.

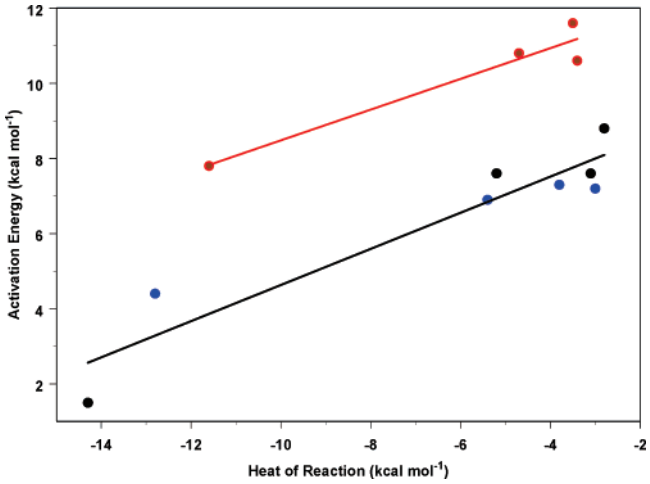

FIGURE 15. Plot of the calculated heats of reaction against the corresponding activation energies for cyclopropane ring-opening reactions. Black symbols give the CBS-RAD data, blue symbols give the QCISD data, and red symbols give the B3LYP data. The black line is the least-squares fit for the B3LYP and CBS-RAD results, the red line for QCISD.

B3LYP/6-31G(d) data, we obtain the following regression formulas:

for cyclopentane ring closures:

$$\Delta E^{*} = 13.05(0.51) + 0.39(0.04)\Delta E_{\text{reaction}} \quad (4)$$

for cyclohexane ring closures:

$$\Delta E^{*} = 18.40(1.19) + 0.39(0.09)\Delta E_{\text{reaction}} \quad (5)$$

for cyclopropane ring openings:

$$\Delta E^{*} = 9.44(0.52) + 0.48(0.07)\Delta E_{\text{reaction}} \quad (6)$$

Equations 4 and 5 suggest that the two alternative ring-closure reactions for the hex-1-ene-5-yl derivatives show essentially the same influence of the heat of reaction on the activation energy (slope) but that the intrinsic barrier for the 5-*exo* ring closure is 5−6 kcal mol^{-1} lower than for the competing 6-*endo* process.

Perhaps not surprisingly, the regression parameters for the cyclopropane ring-opening reactions differ from those for the ring closures. The slope of the correlation is 23% larger than for the other two reactions (i.e., a given change in the heat of reaction has a 23% larger effect on the activation energy), and the intrinsic barrier is roughly half as large as that for the 6-*endo* ring closures.

Thus, the polar effect can be ignored for both types of radical-clock reaction, which are dominated by the enthalpy effect. This suggests that the radical clocks considered will be affected similarly by complexation with metal ions[19,23,24] or other highly charged species.

Acknowledgment. This work was supported by the Deutsche Forschungsgemeinschaft.

Supporting Information Available: Complete tables of the calculated energies and some geometrical features and Gaussian archive entries for the species described. This material is available free of charge via the Internet at http://pubs.acs.org.

JO702421M